Food Chemistry: X 24 (2024) 101940

Contents lists available at ScienceDirect

Food Chemistry: X

journal homepage: www.sciencedirect.com/journal/food-chemistry-x

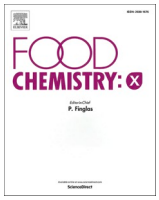

Efficient screening and discovery of umami peptides in Douchi enhanced by molecular dynamics simulations

Weidan Guo [a], Kangzi Ren [a], Zhao Long [a,**], Xiangjin Fu [a,b,*], Jianan Zhang [a], Min Liu [b], Yaquan Chen [c]

[a] College of Food Science and Engineering, Central South University of Forestry and Technology, Changsha 410004, China
[b] Seasonings Green Manufacturing Engineering Technology Research Center of Hunan Province, Hun an Huixiangxuan Bio. Tech. Ltd. Com., Liuyang 410323, China
[c] Hunan Xiangdian Food Ltd. Com, Liuyang 410301, China

ARTICLE INFO

Keywords:
Douchi
Peptidomics
Molecular docking
Molecular dynamics simulation
Umami peptide

ABSTRACT

In this study, a partial least squares discriminant analysis (PLS-DA) discriminant model for umami peptides was constructed based on molecular dynamics simulation data, achieving a R^2 value of 0.949 and a Q^2 value of 0.558. Using this novel model and bioinformatics screening methods, five new umami peptides (EALEATAQ, SPPTEE, SEEG, KEE, and FEE, with umami taste thresholds of 0.139, 0.085, 0.096, 0.060, and 0.079 mg/mL, respectively) were identified in Douchi. Molecular docking revealed that the residues ASN150 of T1R1, as well as SER170, GLU301 and GLN389 of T1R3, might be key amino acid residues for the binding of umami peptides to T1R1/T1R3. Molecular dynamics simulations revealed significant differences in the root-mean-square fluctuation (RMSF) values between the two complex systems of umami peptides-T1R1/T1R3 and non-umami peptides-T1R1/T1R3. The newly constructed umami peptide discriminant model can improve the accuracy of umami peptide screening and enhance the efficiency of discovering new umami peptides.

1. Introduction

Douchi, which originated in China, is one of the traditional fermented foods in East and Southeast Asia (Guo et al., 2023; Guo, Zhang, Long, Fu, & Ren, 2023). It is a well-known traditional condiment in China (Chen et al., 2021; Chen, Wang, Blank, Xu, & Chung, 2021; Wang, Xiang, Zhang, Hou, & Guo, 2021), of which the main taste characteristics consist of umami, sweetness, and saltiness, with umami being the primary one. In previous studies (Guo, Xiao, et al., 2023; Guo, Zhang, et al., 2023), taste peptides have been found to be a crucial compound underlying for the flavor of Douchi, but there are limited studies on identifying associated with umami in Douchi.

Umami peptides are small molecular peptides that exhibit umami characteristics (Li et al., 2022). In recent years, as the concept of healthy food has evolved, consumers' demands for natural foods and ingredients have become increasingly rigorous. Compared to traditional umami enhancers, umami peptides, as a potential new type of umami substance, possess potential the advantages of being natural, safe, and free from side effects (Wang et al., 2023; Wang et al., 2023).

The traditional methods for identifying (Ding, Li, & Kan, 2017) and characterizing (Chen, Li, et al., 2021; Chen, Wang, et al., 2021) umami peptides include multiple steps, such as separation, purification, and assessment, which are not only time-consuming and costly but also have limited accuracy. Recent technological advancements have led to the development of mass spectrometry-based peptidomics technology combined with bioinformatics, molecular docking, and molecular dynamics simulation, which has emerged as a novel, rapid, and effective method for discovering umami peptides, and is gradually gaining widespread acceptance and application (Amin, Kusnadi, Hsu, Doerksen, & Huang, 2020). For example, Jia et al. (2024) have identified three umami peptides in Wuding Chicken, HLEEEIK, LDDALR, and ELY (threshold: 0.03–0.06 mg/mL) using Nano-HPLC-MS/MS-based peptidomics technology combined with sensory evaluation. Through molecular docking and molecular dynamics simulation, they predicted the secondary structures of these peptides, simulated the interactions between the peptides and T1R1/T1R3, and discovered that the TYR74, ARG323 of T1R1, and ARG272, GLN35 of T1R3 are the key amino acid residues for the binding of umami peptides to the receptor. Utilizing

* Corresponding author at: College of Food Science and Engineering, Central South University of Forestry and Technology, Changsha 410004, China.
** Corresponding author.
E-mail addresses: longzhao@csuft.edu.cn (Z. Long), drxjfu@163.com (X. Fu).

https://doi.org/10.1016/j.fochx.2024.101940
Received 13 September 2024; Received in revised form 24 October 2024; Accepted 28 October 2024
Available online 29 October 2024

Table 1
Taste information on umami and non-umami amino acids and peptides used for modeling.

Sequence	Taste	Umami threshold ($mg \cdot mL^{-1}$)
E	umami	0.300
DD	umami	1.410
EE	umami	0.068
EGS	umami	1.135
NNP	umami	0.140
AAPY	umami	0.887
GGGE	umami	0.589
EEDGK	umami	0.811
LPEEV	umami	2.000
ALPEEV	umami	0.186
TESSSE	umami	0.142
HLQLAIR	umami	0.575
SEASNNK	umami	0.23
HGEDKEGE	umami	0.143
SLAKGDEE	umami	0.283
LLLPGELAK	umami	0.315
STMLLESER	umami	0.754
AGFAGDDAPR	umami	0.283
GYSFTTTAER	umami	1.461
VLPTDQNFILR	umami	0.125
DAGVIAGLNVLR	umami	0.284
RGENESEEEGAIVT	umami	0.125
R	non umami	–
GL	non umami	–
RRPFF	non umami	–
YPFPFPIPN	non umami	–

–: No threshold was reported in literature.

peptidomics and machine learning methods, Wang et al. (2024) identified 16 umami peptides (threshold: 0.09–0.35 mg/mL) from fermented sea bass. Through molecular docking, it was discovered that these 16 peptides formed stable complexes with the T1R3 protein, with key binding sites including SER170, SER147, GLN389, and HIS145. The primary interaction forces were aromatic interactions and hydrogen bonds. However, most of the current research focuses on static analysis methods, such as molecular docking. There are few studies on the umami peptides by dynamic analysis tools such as molecular dynamics simulation (MD Simulation), and few literatures have summarized their umami regularity.

The objectives of this study were: 1) to investigate the structure-activity relationships of umami receptors and ligands via MD Simulation, in order to elucidate umami perception mechanism. 2) to establish guidelines for screening umami peptides by MD Simulation, molecular docking and bioinformatics analysis to enhance the accuracy of their identification. To accomplish these goals, The taste properties of three types of Chinese Douchi were analyzed using an electronic tongue. Non-targeted broad-spectrum detection of endogenous peptides in Douchi was performed using LC-MS/MS-based peptidomics technology. A new discriminant model for umami peptides was established based on molecular docking and MD Simulation data. Combining bioinformatics analysis, new umami peptides in Douchi were identified.

2. Materials and methods

2.1. Samples

The project collected a total of 12 samples of three common types of Douchi (*Aspergillus-type*: Liuyang Douchi, Yangjiang Douchi, and *Mucor-type*: Yongchuan Douchi) in the Chinese market. Each type of Douchi includes four sub-samples from different brands. The Douchi samples were purchased from local supermarkets. Douchi were ground into powder in liquid nitrogen and stored at −20 °C before use.

2.2. Methods

2.2.1. Construction of a discrimination model for umami peptides based on molecular dynamics simulation data

2.2.1.1. Homology modeling of receptor structure. T1R1/T1R3, the primary receptor for umami taste, belongs to class C of G protein-coupled receptors and comprises three parts: the extracellular venus flytrap domain (VFT), the intracellular transmembrane helix domain (TMD), and the *Cysteine-rich* domain (CRD) connecting above two domains.

The AlphaFold2 2.3.0 (Wayment-Steele et al., 2024) multimer module was employed to perform homology modeling and structural optimization of the umami receptor T1R1/T1R3. The optimal conformation was then selected for a 50 ns MD, and the final stable conformation was retained for subsequent research.

The Ramachandran Plot of the homology modeling revealed that over 99.9 % of the points in the T1R1/T1R3 receptor model fell within the reasonable region, and the amino acid residues maintained a good conformational space. Among them, 93.6 % were located in the most favorable region, 6.4 % in the additional allowed region, and only 0.1 % of the amino acid residues were in the generously allowed region (Fig. S1). The umami receptor structure obtained through homology modeling is considered reasonable and complete, which can be used to study the relationship between umami peptides and T1R1/T1R3.

Five active pockets in T1R1/T1R3 were predicted using POCASA prediction platform (http://altair.sci.hokudai.ac.jp/g6/service/pocasa/), and the most active binding domain was found to be the VFT (Li et al., 2021). The VFT and CRD of T1R1/T1R3 (T1R1: 1-564; T1R3: 1-566) were extracted and were used to perform molecular docking and dynamics simulations.

2.2.1.2. Data sets for modeling. Twenty six peptides (Table 1) with varying lengths and known thresholds were selected from the databases. Among them, twenty two umami sequences were from BIOPEP-UWM and the Flavor Database of umami peptides, and four non-umami sequences were from BIOPEP-UWM and literature reports (Liu et al., 2023), with clear artificial sensory thresholds and literature support, respectively.

2.2.1.3. Molecular docking. Preparation of Ligands: The PEP-FOLD3 (https://bioserv.rpbs.univ-paris-diderot. fr/services/PEP-FOLD3/) online simulation platform (Zhao et al., 2020) was utilized to construct the three-dimensional structure of peptide molecules and stored in PDB format (Shen, Maupetit, Derreumaux, & Tufféry, 2014).

Docking Parameters: The Autodock 1.4.7 was employed to dock the umami receptor structure with umami peptides. The docking was centered on the T1R1/T1R3-VFD (X center = 37.288, Y center = 48.507, Z center = 36.614), with the box dimensions of Size X = 80, Size Y = 126, Size Z = 88 (large enough to accommodate the binding pocket region of T1R1/T1R3-VFD) (Seifert et al., 2016).

Twenty conformations and scores were generated for each docking run, and the resulting conformations were ranked based on binding energy scores. The best-docked conformation was selected for the following studies.

2.2.1.4. Molecular dynamics simulation (MD simulation). MD Simulation was performed using GROMACS 2023.2 software (Smith, Dong, & Raghavan, 2022). The topology of the T1R1/T1R3-peptide (complex) was generated using the Generalized Amber Force Field (GAFF).

The size of the simulation box was optimized to ensure that each atom of the protein was more than 1.0 nm away from the box. Then, the box was filled with H_2O (transferable interatomic potential with three points model, TIP3P Water Model) at a density of 1 g/cm^3. Subsequently, some water molecules were replaced with Cl^- or Na^+ ions to ensure that the simulation system was electrically neutral.

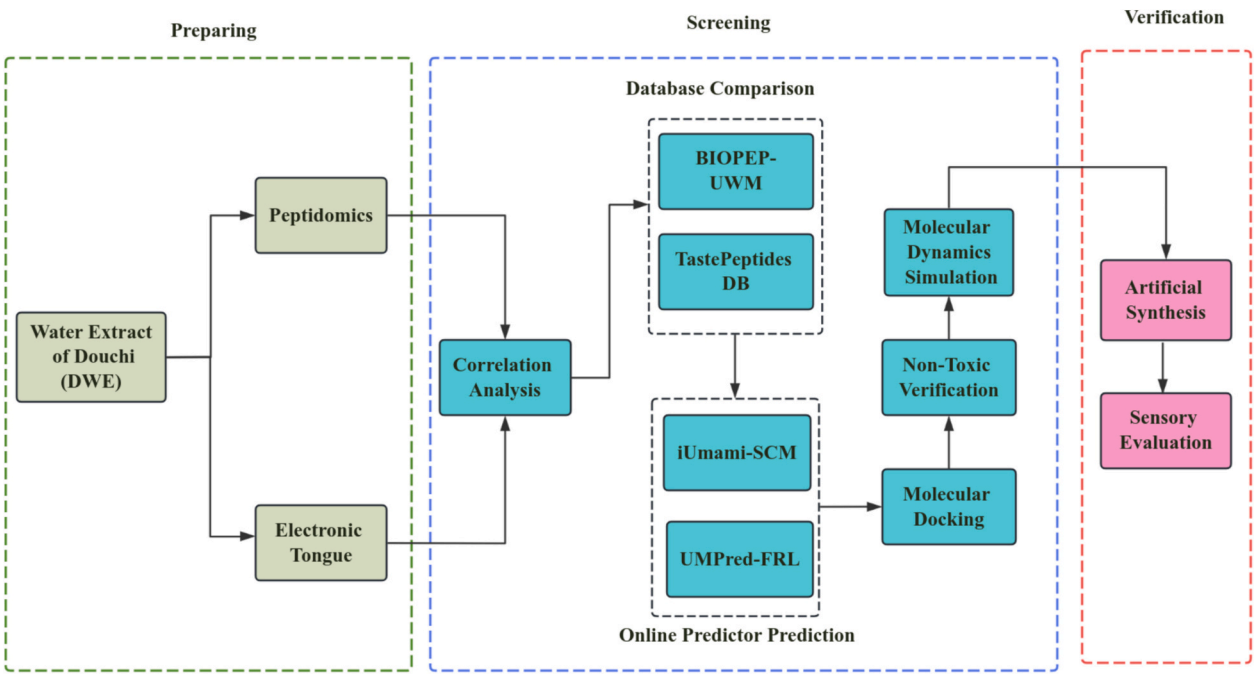

Fig. 1. Flowchart for rapid screening of umami peptides in Douchi.

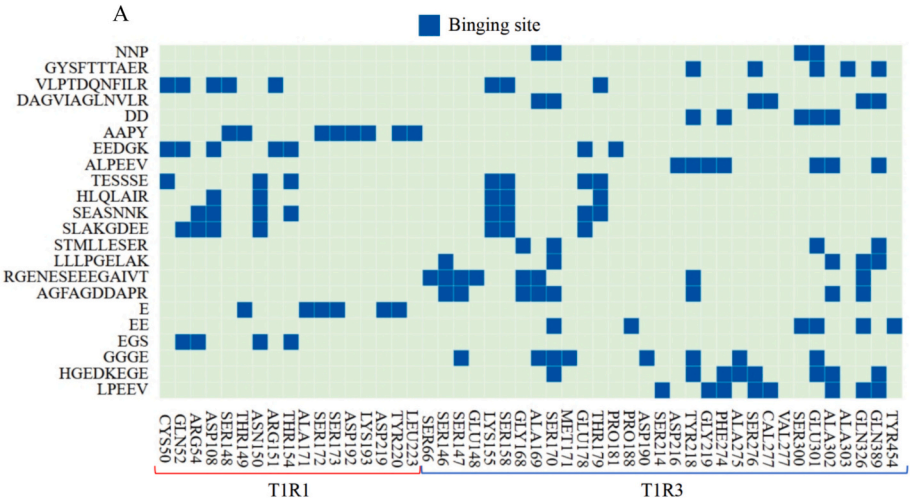

Fig. 2. Structural variations in the complex systems of T1R1/T1R3 with umami or non-umami peptides.
A: Distribution of binding sites of umami peptide to T1R1/T1R3.
B: Comparison of mean RMSF trajectories from MD Simulations (graphing amino acids within residues 1–550 of the VFT + CRD sections), with complete RMSF data presented in Fig. S4, S5.
C: Final structures of T1R1/T1R3 after MD Simulations.
Green represents the protein structure without ligand binding, red represents the umami peptide-receptor complex, and blue represents the non-umami peptide-receptor complex. (For interpretation of the references to colour in this figure legend, the reader is referred to the web version of this article.)

Energy minimization was carried out using the steepest descent method to reduce unreasonable contacts or atomic overlaps in the entire system. After energy minimization, the simulation system was pre-equilibrated using the NVT module and the NPT module respectively at 300 K. Finally, dynamic simulations were conducted. The stable conformations, and root-mean-square fluctuations (RMSF) were collected.

2.2.1.5. PLS-DA discriminant model for umami peptides based on MD simulation data. The RMSF values obtained from 15 ns of MD Simulation was used as the dataset, a partial least squares discriminant analysis (PLS-DA) model was established using SIMCA 14.1 software (Umetrics, Sweden).

The identification of differential amino acid residues was identified by the following rule: the ones with fold change (FC) values greater than 1.5 or less than 0.67, and *p*-values less than 0.05 in the PLS-DA model were screened as differential amino acids.

2.2.1.6. Analysis of Douchi umami peptides using the discriminant model based on MD simulation data. The RMSF values obtained from the MD Simulation of the peptide-T1R1/T1R3 complex system were imported into the PLS-DA model as predictor variables, and the specify module of

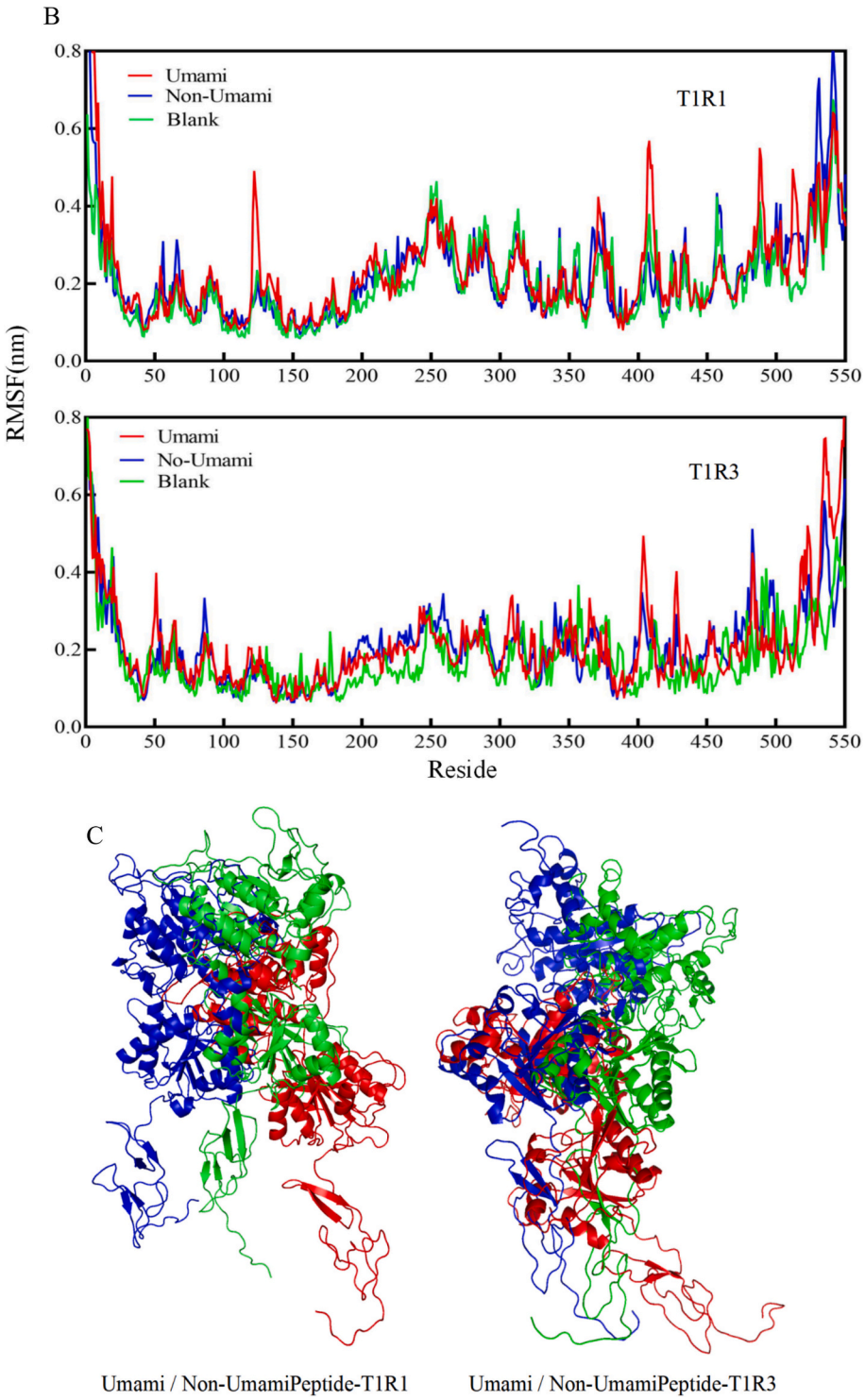

Fig. 2. (*continued*).

SIMCA was used for validation. Peptide sequences located below the DCrit (0.05) line, indicating a 95 % confidence interval, in the DModXPS+ plot were identified as umami peptide sequences with umami properties.

2.2.2. *Rapid screening of Douchi umami peptides*

The rapid screening of Douchi umami peptides comprises the following eight steps (Fig. 1):

1) Peptidomics analysis of Douchi based on LC-MS/MS.
2) Correlation analysis between the content of Douchi peptides and the umami taste detected by an electronic tongue (Fig. S2). The sequences that showed significant positive correlations were retained.
3) Comparison with umami databases (Iwaniak, Minkiewicz, Darewicz, Sieniawski, & Starowicz, 2016): BIOPEP-UWM (www.uwm.edu.pl/biochemia) and Flavor Database (https://mffi.sjtu.edu.cn/ database). The sequences not reported by the database were retained.
4) Prediction using online umami peptide predictors: iUmami-SCM (https://cam t.pythonanywhere.com/iUmami-SCM) and UMPred-FRL

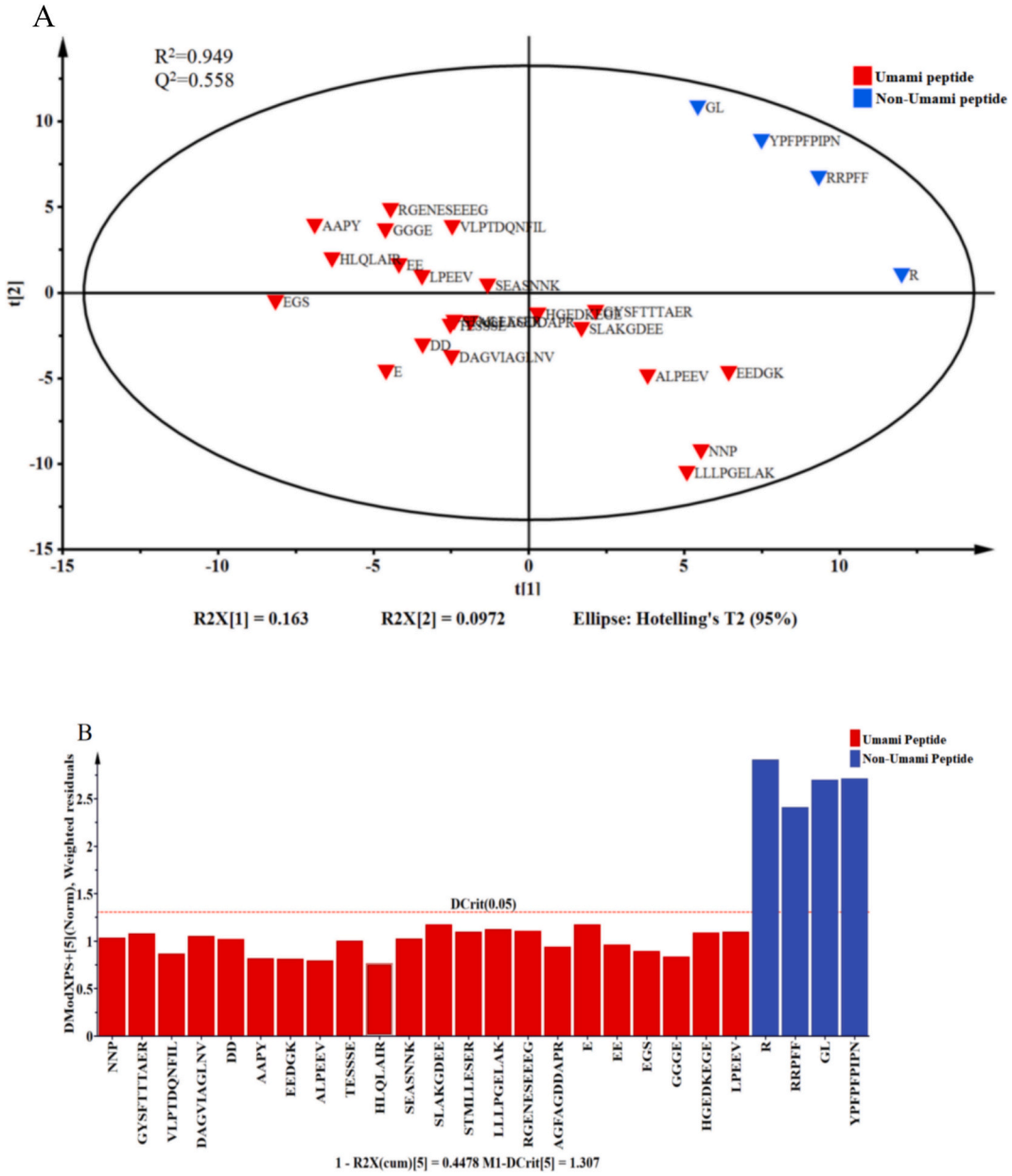

Fig. 3. Construction of an umami peptide prediction model based on RMSF data from MD Simulations.
A: Score plot of the umami peptide prediction model.
B: Internal validation of the umami peptide model (DModXPS+ plot). Weights below the DCrit(0.05) line indicate umami, represented in red; those above the line indicate non-umami, represented in blue.
C: Cross-validation plot of the umami peptide prediction model.
D: Box plot of significant amino acid difference sites indicated by RMSF (data with FC > 2 or FC < 0.5 and $p < 0.01$). (For interpretation of the references to colour in this figure legend, the reader is referred to the web version of this article.)

(http://pmlabstack.pythonan ywhere.com/UMPred-FRL). The peptides predicted as umami on both platforms were retained.
5) After molecular docking, the peptides with binding energies lower than the positive control were retained (the binding energy between L-glutamic acid and T1R1 -VFT).
6) After toxicity screening, predicting the toxicity of peptides using ToxinPred (https: //webs.iiitd.edu.in/raghava/toxinpred/design.php) and the sequences predicted to have potential toxicity to humans were eliminated.
7) In PLS-DA umami peptide discrimination model analysis.
8) The peptides were artificially synthesized and subjected to sensory evaluation.

2.2.3. LC-MS/MS peptidomics analysis of Douchi

Twenty mg of Douchi powder sample was taken into an EP tube, and 2 mL of 1 % formic acid was added. The mixture was vortexed until evenly mixed followed by sonicated in ice for 10 min. The mixture was centrifuged at 20,000*g* for 30 min at 4 °C (TG25KR, Dongwang Instruments, Changsha, China). The supernatant was collected as the test solution and stored at 4 °C for analysis using the EASY-nLC 1000 ultra-high-pressure nano-liquid chromatography system (Thermo Scientific, USA).

The LC conditions: liquid phase A was 0.1 % formic acid-water solution, and liquid phase B was 0.1 % formic acid-acetonitrile solution. Separation of sample was executed with a 60 min gradient at 300 nL/

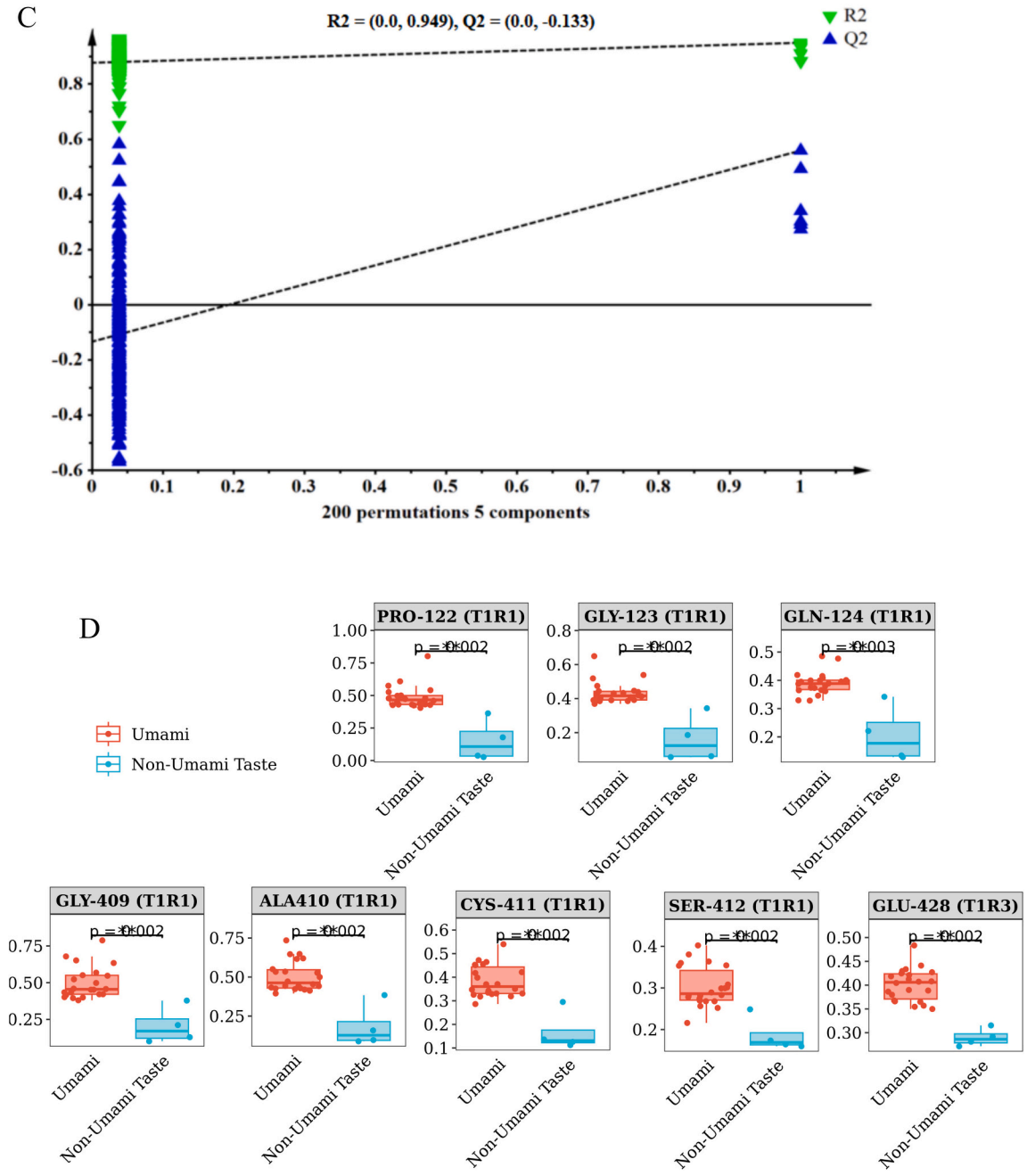

Fig. 3. (*continued*).

min flow rate. Gradient B: 2–5 % for 2 min, 5–22 % for 34 min, 22–45 % for 20 min, 45–95 % for 2 min, 95 % for 2 min. (Garshick et al., 2019).

MS conditions: The ion source spray voltage was set to 2.2 kV, and the heating capillary of the fusion mass spectrometer was set to 320 °C. Data-dependent acquisition was used to automatically switch between MS and MS/MS (Lee et al., 2016).

MaxQuant software (version 1.6.5.0) was used to search the liquid chromatography-mass spectrometry raw files. The quantitative analysis was conducted by iBAQ algorithm using MaxQuant software.

2.2.4. Artificial synthesis of peptides and determination of their taste characteristics and thresholds

The selected peptide sequences were artificially synthesized by ChiaPeptides Co., ltd. (Shanghai, China) using FMOC solid-phase chemical synthesis (Guo, Xiao, et al., 2023; Guo, Zhang, et al., 2023).

Eleven panelists of the sensory evaluation (6 females and 5 males, aged 24–30 years) with sensory evaluation experience were recruited from the College of Food Science and Engineering, Central South University of Forestry and Technology (Changsha, China). Four-week sensory training was conducted for 11 trained sensory evaluators on the five basic tastes of sourness, sweetness, bitterness, saltiness, and umami, referring to the National Standard of China (GB/T 16291.1-2012). Prior to their participation, each team member has signed an informed consent to participate in the study, and the process strictly follows the guidelines outlined in the Declaration of Helsinki, ensuring the study conforms to ethical norms. This study has been reviewed and approved by the relevant audit institutions and committees of the college (Appendix 2 - Informed Consent for the Sensory evaluation).

The analysis of taste characteristics and threshold determination of synthetic peptides were performed referring to the methods of Su et al.

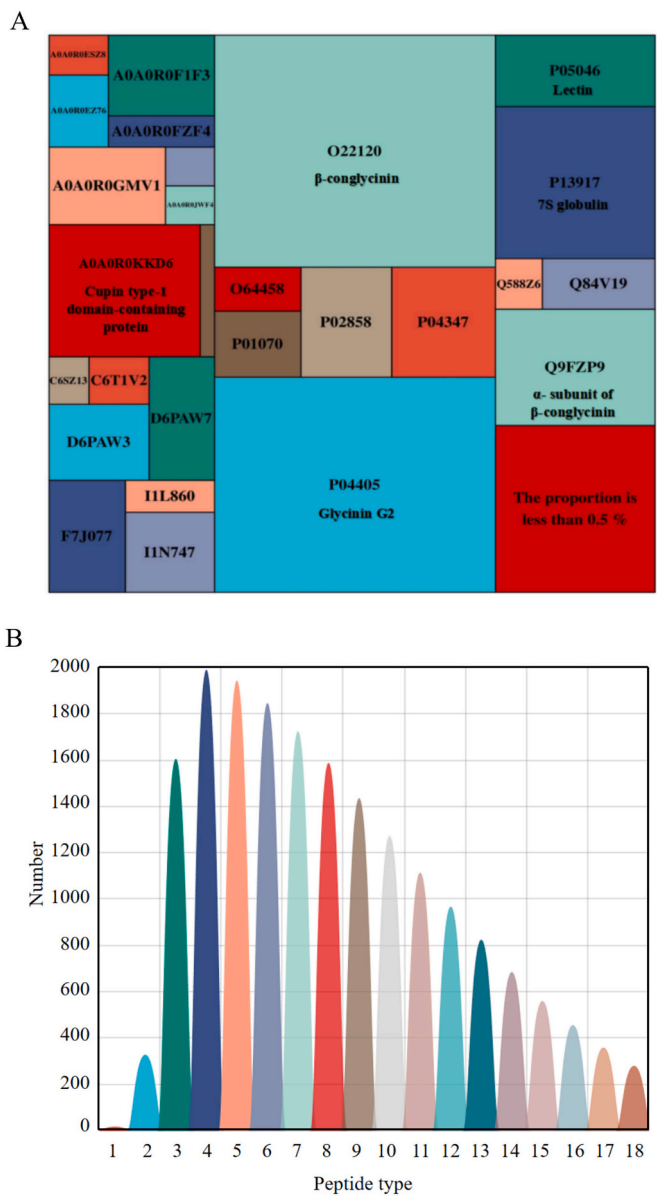

Fig. 4. Profile analysis of Douchi peptidomics.
A: Tree Diagram showing the proportional distribution of Douchi peptidomics precursor proteins, with area size representing the degree of proportional occupancy.
B: Distribution of peptide lengths in Douchi.

(2023). The synthetic peptides were dissolved in ultrapure water at a concentration of 2 mg/mL and then mixed using a vortex mixer for 30 s. They were randomly assigned three-digit numbers for sensory evaluation. The evaluators need to describe umami, sweetness, sourness, saltiness and bitterness of the samples.

The triangle test (2 blank water samples, 1 peptide solution) was used to distinguish each diluted level. The samples were diluted with ultrapure water at a ratio of 1:1 (*v*/v). Each level of sample was measured using a three-point method at 30 °C for sensory evaluation. The mean value of the final two dilution concentrations that effectively differentiated the taste between the synthetic peptide solution and the water samples was recorded as the individual umami recognition threshold-dilution value (TD). The final value was determined by averaging the results of three separate experiments.

2.2.5. Data analysis

Data collation and correlation analysis were conducted using Excel and SPSS 22.0 (SPSS Inc., Chicago, IL, USA), with $p < 0.05$ indicating significant differences. Graph plotting was completed with Origin 2018 (OriginLab Corporation, Northampton, MA, USA). For the results of molecular docking and MD Simulation, visualization analysis and interaction analysis were performed using Pymol 2.4.0 (Schrödinger Inc., USA). The twodimensional (2D) diagram of the docking results was presented by Discovery Studio (DS) 2019 (BIOVIA, Dassault Systèmes, San Diego) (Singh, Upadhyay, & Reddy, 2021).

3. Results and discussion

3.1. Construction of umami peptide discrimination model based on MD simulation data

Umami and bitter amino acids exhibit significant differences in chemical structure and properties (Liu, Da, & Liu, 2019), which may lead to distinct conformational and dynamic characteristics when they interact with the umami receptor T1R1/T1R3 in MD Simulation.

In order to elucidate umami perception mechanism, this study selected 26 sequences of varying peptide lengths with known thresholds from the database (Table 1), including 22 umami peptides or amino acid and 4 non-umami peptides (Liu et al., 2023). After molecular docking, MD were performed for 15 ns.

When umami peptides bind to T1R1/T1R3, they interact with amino acid residues in the VFT binding domain of T1R1/T1R3 through hydrogen bonds. Specifically, the amino acid residues involved were (for the T1R1 subunit): CYS50, GLN52, ARG54, ASP108, SER148, THR149, ASN150, ARG151, THR154, ALA171, SER172, SER173, ASP192, LYS193, ASP219, TYR220, and LEU223; and for the T1R3 subunit: SER66, SER146, SER147, GLU148, LYS155, SER158, GLY168, ALA169, SER170, MET171, GLU178, THR179, PRO181, PRO188, ASP190, SER214, ASP216, TYR218, GLY219, PHE274, ALA275, SER276, CAL277, VAL277, SER300, GLU301, ALA302, ALA303, GLN326, GLN389, and TYR454 (Fig. 2A). Among them, ASN150 showed high docking frequency, indicating that it significantly impacted the binding region of T1R1. Meanwhile, SER170, GLU301 and GLN389 of T1R3 also exhibited a high occurrence frequency. It is speculated that these four amino acid residues might be the key amino acid residues for the binding of umami peptides to T1R1/T1R3. In the umami peptiede-T1R1/T1R3 system, the frequency of SER, GLN, ALA and GLU in the binding sites exceeded 50 %, and the frequency of SER was the highest, reaching 23.24 %. GLU is a negatively charged polar amino acid and a strong hydrogen bond acceptor amino acid. SER is a common hydrophilic amino acid. It contains polar hydroxyl groups, which generally distribute on the surface of globular proteins (Rapino et al., 2021). It has been reported that in chicken soup, SER promotes the formation of 83 % umami peptide-T1R3 complex (Cui et al., 2023; Cui, Li, Wu, & Hu, 2023). The above result is consistent with the report that SER and GLU might be the key residues for the binding of umami peptides to T1R1/T1R3 (Feng et al., 2024; Li et al., 2022; Wang, Wang, Xu, et al., 2023; Wang, Wang, Zhang, et al., 2023; L. Zhang et al., 2023).

The statistical analysis revealed that the binding of 22 umami peptides to T1R1/T1R3 could be categorized into three types: binding to the cavity of the umami receptor T1R1 (E, EGS, AAPY), embedding into the binding pocket of the T1R3 cavity (NNP, GYSFTTTAER, DAGVIAGLNVLR, DD, ALPEEV, STMLLESER, LLLPGELAK, RGENESEEEGAIVT, AGFAGDDAPR, EE, GGGE, HGEDKEGE, LPEEV), and interacting with both T1R1 and T1R3 (VLPTDQNFILR, EEDGK, TESSSE, HLQLAIR, SEASNNK, SLAKGDEE). This classification aligns with the summarized patterns of 11 peptides identified by Fu et al. (2024) and Yang, Fu, Meng, Liu, and Bi (2024) et al. in Agaricus blazei and watermelon soybean paste. For instance, among the 11 umami peptides in *Agrocybe aegerita*, four (EY, EG, ECG, and DGPL) were located in the cavity of the umami receptor T1R1, four (EV, ENG, DEL, and EDCS) were embedded

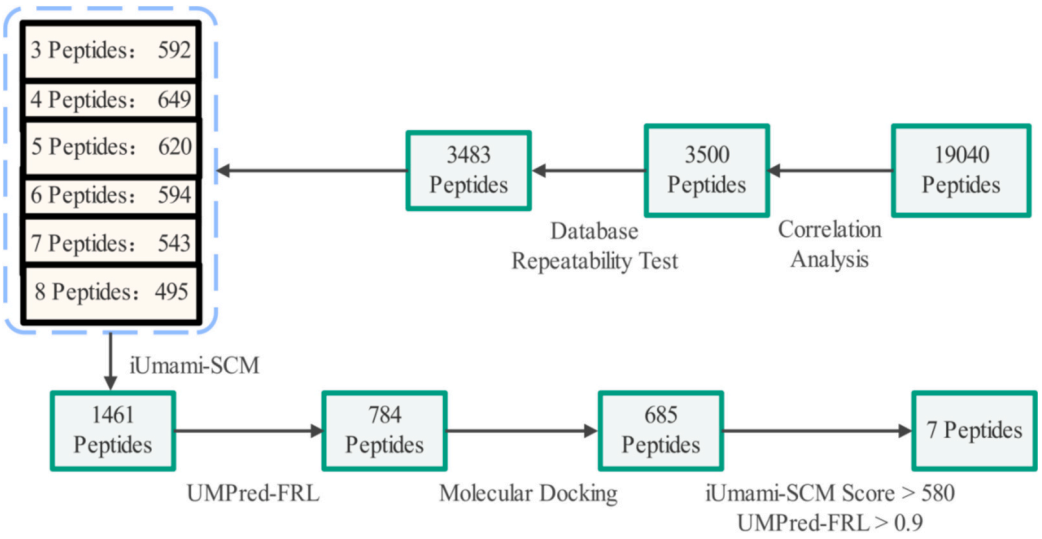

Fig. 5. Workflow of peptide screening and analysis in Douchi peptidomics.

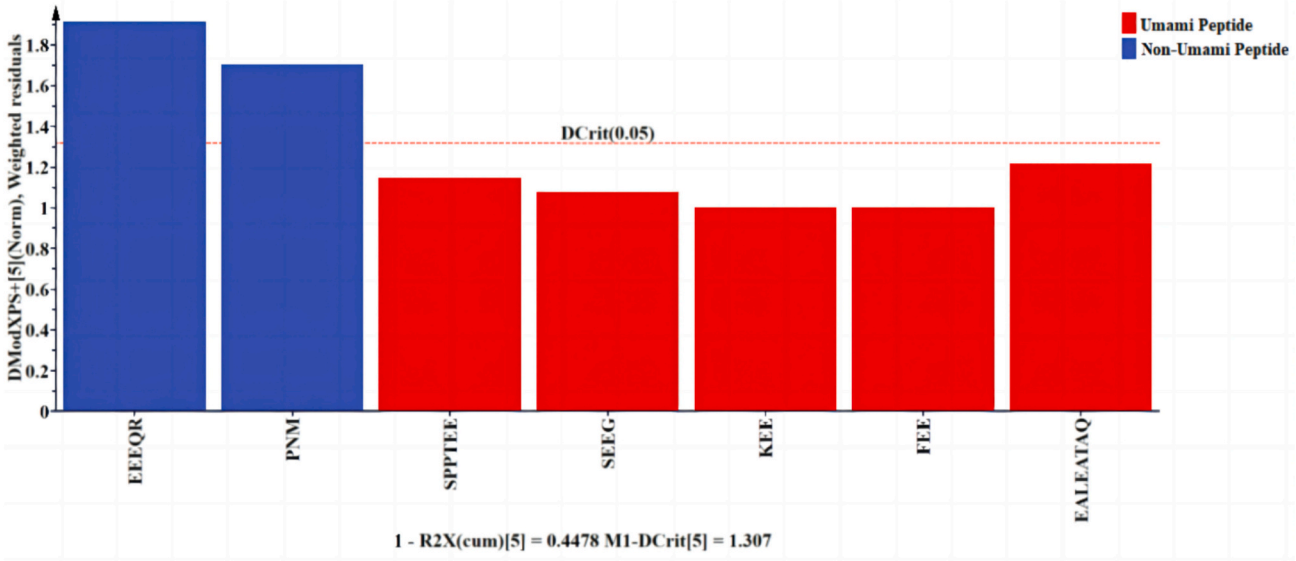

Fig. 6. The umami peptides in Douchi were identified and verified by the weighted sum of squared residuals (DModXPS+). Weights below the DCrit(0.05) line indicate umami, represented in red; those above the line indicate non-umami, represented in blue. (For interpretation of the references to colour in this figure legend, the reader is referred to the web version of this article.)

Table 2
Taste characteristics of synthetic peptides.

Number	Sequence	iUmami-SCM	UMPred-FRL	MD*	Bind energy (kcal·mol^{-1})	Taste	Umami threshold (mg·mL^{-1})
1	EALEATAQ	+	+	+	−7.5	umami	0.139
2	SPPTEE	+	+	+	−6.1	umami	0.085
3	SEEG	+	+	+	−5.5	umami	0.096
4	KEE	+	+	+	−5.3	umami	0.060
5	FEE	+	+	+	−5.3	umami, salty	0.079
6	PNM	+	+	−	−5.3	n.d.	n.d.
7	EEEQR	+	+	−	−5.8	sweet	n.d.

+: The predicted result is umami.
−: The predicted result is non-umami.
n.d.: No detected.
* : The umami peptide prediction model constructed in present study based on RMSF data from MD simulations.

in the binding pocket of the T1R3 cavity, and the remaining three (PEG, DDL, and PEEL) strongly interacted with both T1R1 and T1R3.

Furthermore, there is a specific pattern in the distribution of binding regions: The receptor T1R1 cavity mainly accommodates small peptides composed of 1 to 4 amino acid residues. However, there is no specific length or sequence limitation for the T1R3 region and the T1R1/T1R3

composite cavity region when binding peptides. Some peptides with a length greater than 5 or more amino acids can bind to the T1R3 region or the T1R1/T1R3 composite cavity. For example, three new umami tetrapeptides identified by Zhao et al. (2023) in rainbow trout bind to the binding pocket of the T1R1 cavity, while 13 long peptides (5–14 amino acids) identified by Du and Zhang in Pacific oyster (*Crassostrea gigas*) and Termitomyces albuminosus bind to the T1R3 (Fu et al., 2024; Zhang et al., 2024; Zhang, Tu, Wen, Wang, & Hu, 2024). These research findings further validate the pattern that umami peptides of different lengths might have different acting sites.

From the analysis of the mean RMSF trajectories (Fig. 2B) and the visualization analysis of the final structures of protein binding with peptides (Fig. 2C), it can be observed that upon binding of ligands with different taste characteristics to the T1R1/T1R3, there are shifts in the amino acid positions of the VFT. Specifically, these shifts are observed at the following significant sites (T1R1: MET1, LEU8, PHE21, ARG56, PRO57, PRO122, GLY123, GLN124, SER137, GLU366, GLN368, LYS379, SER382, LEU403, SER408, GLY409, ALA410, CYS411, SER412, GLY458, PRO459; T1R3: LEU51, VAL309, ASN406, THR407, GLU428, MET430). Furthermore, these displacements propagate further to the C-terminal domain (CRD), leading to changes in consecutive amino acids in the CRD. Notably, in T1R3, due to its larger cavity, the displacements are more significant, manifesting in the regions PRO495-SER497 and PHE540-GLU545. The results showed that the changes of amino acids were more consistent from the VFT region to the CRD region. A possible scenario is that the consistent change could lead to a rearrangement of amino acid positions in the TMD. Ultimately, this might result in the movement or even swapping of helices, transmitting the umami signal.

The hypothesis is consistent with the rule of protein conformation changes after the activation of other G protein-coupled receptors (GPCRs) (Wang, Wang, Xu, et al., 2023; Wang, Wang, Zhang, et al., 2023). Metabotropic glutamate receptors (mGluRs), as a member of the C-type G protein-coupled receptor (GPCR) family, have been widely studied for their protein conformation changes during activation. During the activation process, these receptors undergo a signal transfer between the Venus Flytrap domain (VFT), the Cysteine-Rich Domain (CRD), and the Transmembrane Domain (TMD), which comprises seven transmembrane helices. First, the Venus flytrap (VFT) domain outside the membrane binds to an activating ligand, leading to a decrease in the distance between the upper and lower lobes of the VFT, and rearrangement of the hinge region between the upper and lower lobes at the dimer interface (Krishna Kumar et al., 2024). Subsequently, this change causes the CRD and the TMD connected to move closer to each other. Within TMD, the TM4 of two subunits forms a tight interaction, while the TM6 forms a shallow groove via its intracellular loop region, binding to the C-terminus of the G protein (Du et al., 2021; Lin et al., 2021). This combination ultimately activates a series of downstream physiological activities.

In Fig. 2B, the mean RMSF trajectories obtained from MD Simulation of the peptide-T1R1/T1R3 complexes are compared with that of ligand-free T1R1/T1R3. To highlight the contrast in detail, Fig. 2B specifically emphasizes the trajectory changes of the first 550 amino acids of T1R1 and T1R3. For umami peptides, there are 24 significantly different sites ($p < 0.01$) in T1R1. Meanwhile, 98 sites ($p < 0.01$) exhibit significant differences in T1R3. For non-umami peptides, there are 60 significantly different sites ($p < 0.01$), with 6 located in T1R1 and 54 in T1R3.

By analyzing the statistical results of these differential sites, it could be observed that in the complex system with ligands, the impact of ligand binding on T1R3 was greater than that on T1R1. This might be due to the fact that T1R3, compared to T1R1, possesses a larger open cavity domain (Liu et al., 2023), which allows the protein to have a higher degree of freedom of movement.

The RMSF values were taken as the dataset (Fig. S3, S4). Partial least squares discriminant analysis (PLS-DA) was employed to establish an umami peptide discrimination model (Fig. 3).

The model results indicate that the 26 peptides can be accurately classified into umami and non-umami categories, with complete accuracy (Fig. 3A, B). The model's R^2 value is 0.949, and Q^2 is 0.558 (Fig. 3C), suggesting that the model is valid according to the established criteria (Yan et al., 2024).

A total of 39 amino acid residues with significant changes ($p < 0.05$, FC > 1.5 or < 0.67) in RMSF were identified: MET1, LEU8, PHE21, ARG56, PRO57, PRO122, GLY123, GLN124, SER137, GLU366, GLN368, LYS379, SER382, LEU403, SER408, GLY409, ALA410, CYS411, SER412, GLY458, PRO459, ASN490, GLN491, TYR534 of T1R1; and LEU51, VAL309, ASN406, THR407, GLU428, MET430, PRO495, VAL496, SER497, PHE540, CYS541, GLY542, GLN543, ASP544, GLU545 of T1R3. Among these, 27 are in the VFT domain, and 12 are in the CRD domain. Eight amino acid residues with FC > 2 or FC < 0.5 and $p < 0.01$ were chosen for presentation. These include PRO122, GLY123, GLN124, GLY409, ALA410, CYS411, and SER412 of T1R1, as well as GLU428 of T1R3 (Fig. 3D).

3.2. Analysis of the peptide profiles of Douchi

Through non-targeted peptidomics methods, a total of 19,040 peptide sequences were obtained from 12 Douchi samples.The chromatogram of total ion current is shown in Fig. S6. Analysis of their precursor protein types revealed 60 categories, with glycinin G2 (P04405) and β-conglycinin (O22120) as the major components (Fig. 4A). Glycinin G2 and β-conglycinin are two major soy proteins, accounting for 70–80 % of the total seed globulin content. Studies have shown that during soybean fermentation, the α-subunit of β-conglycinin and glycinin G2 undergo specific degradation, with hydrolytic sites located on the molecular surface or in mobile disordered regions (Shirotani et al., 2021). Analysis of peptide length revealed that tetrapeptides are the most abundant, followed by pentapeptides (Fig. 4B).

3.3. Bioinformatics analysis of the Douchi Peptidomics

To enhance the accuracy of umami peptide identification, the rapid screening of Douchi umami peptides was optimized (Fig. 5).

The correlation between the content of Douchi peptide and the umami value in the sensory results of Douchi was analyzed (data not shown). A total of 3500 peptide sequences with a significant positive correlation ($p < 0.05$) with the umami value of Douchi and a length of 3–8 amino acids were screened and retained.

After comparing with the sequences in the BIOPEP-UWM database (www.uwm.edu.pl/biochemia), 17 previously reported umami peptides (AEA, DDE, DED, DEE, EDE, EDV, EED, EEE, EGS, EPQ, GFP, LDL, NNP, PET, SEE, LPEEV, ALPEEV) were excluded, leaving 3483 peptides, including 592 tripeptides, 649 tetrapeptides, 620 pentapeptides, 584 hexapeptides, 543 heptapeptides, and 495 octapeptides for further screening.

These sequences were then subjected to prediction using the machine learning-based iUmami-SCM and UMPred-FRL online umami peptide prediction platforms. Of these, 784 peptides predicted to be umami-taste by both platforms were selected for batch molecular docking with T1R1/T1R3.

We retained those peptides with molecular docking binding energies lower than the glutamic acid binding energy (−5.2 Kcal) and screened out the peptide sequences without toxicity using the ToxinPred webserver algorithm, resulting in a total of 685 peptides.

Finally, the remaining peptides were sorted according to their scores on the online umami peptide prediction platforms. Seven peptide sequences with iUmami-SCM scores greater than 580 (Zhang, Tu, et al., 2024; Zhang, Zhang, et al., 2024), UMPred-FRL scores greater than 0.9 (Cui, Li, et al., 2023; Cui, Zhang, et al., 2023), and ranked within the top 80 in both platforms were selected.

Through the rapid bioinformatics screening described above, we have identified a total of seven novel potential umami peptides in Douchi, which are EALEATAQ, SPPTEE, SEEG, KEE, FEE, PNM, and

EEEQR (Fig. 5).

3.4. Analysis of potential umami peptides in Douchi using the PLS-DA umami peptide discrimination model and verification of their artificial synthesis

The seven potential umami peptides rapidly screened through bioinformatics analysis undergone MD Simulation, and the RMSF results were substituted into the PLS-DA model for classification. It was found that according to the PLS-DA model, five peptides were predicted to be umami peptides, and two were predicted to be non-umami (Fig. 6).

Finally, all seven peptides were artificially synthesized, and sensory evaluations were conducted to determine the umami threshold (Table 2). The results of the taste characteristics of these peptides determined by sensory evaluation are consistent with the classification results of the PLS-DA model. The five predicted umami peptides showed threshold between 0.060 and 0.150 mg/mL, all of which were lower than the umami threshold of 0.3 mg/mL for sodium glutamate. Among them, KEE (threshold: 0.060 mg/mL; binding energy: −5.3 kcal/mol) had the strongest umami taste. It has a stronger umami characteristic than the umami peptides in yeast extract and Pacific oyster ethanol extract reported in the literatures (Fu et al., 2024; Jia et al., 2024; Wang, Wang, Xu, et al., 2023; Wang, Wang, Zhang, et al., 2023). This result verifies the validity of the model.

4. Conclusion

Five novel umami peptides were identified in Douchi, with a threshold range of 0.060 to 0.150 mg/mL. The PLS-DA discriminant model constructed for umami peptides exhibited an R^2 value of 0.949 and a Q^2 value of 0.558. The residues ASN150 of T1R1, as well as SER170, GLU301 and GLN389 of T1R3, were suggested as the key amino acid residues for the binding of umami peptides to the T1R1/T1R3 receptor complex. Furthermore, it was found that the amino acid residues with significant RMSF changes are concentrated in the T1R3. A total of 39 different amino acid sites of the two complex systems formed by umami/non-umami peptides and the taste receptor proteins (T1R1/T1R3) were identified. From the VFT to the CRD, it was observed that the amino acid site shift of the protein changed from occasional to continuous and cumulative. This phenomenon might potentially represent the initial signaling of umami taste perception.

CRediT authorship contribution statement

Weidan Guo: Writing – original draft, Visualization, Supervision, Methodology. **Kangzi Ren:** Writing – original draft, Formal analysis. **Zhao Long:** Writing – review & editing, Supervision, Project administration. **Xiangjin Fu:** Writing – review & editing, Supervision, Project administration, Funding acquisition, Conceptualization. **Jianan Zhang:** Writing – original draft, Conceptualization. **Min Liu:** Resources. **Yaquan Chen:** Resources.

Declaration of competing interest

The authors declare that they have no known competing financial interests or personal relationships that could have appeared to influence the work reported in this paper.

Data availability

No data was used for the research described in the article.

Acknowledgment

Thanks the support of the National Key Research and Development Program of China (No. 2022YFD2101303), and Science and Technology Innovation Project for Graduate Students of “Keming Foods”: (2023KMCX03).

Peptidomics analysis was assisted by Biotree Biotech Co., Ltd. (Shanghai, China). Electronic tongue analysis was assisted by Keming Noodle Manufactuing Co.,Ltd. (Changsha, China).

Appendix A. Supplementary data

Supplementary data to this article can be found online at https://doi.org/10.1016/j.fochx.2024.101940.

References

Amin, M. N. G., Kusnadi, J., Hsu, J.-L., Doerksen, R. J., & Huang, T.-C. (2020). Identification of a novel umami peptide in tempeh (Indonesian fermented soybean) and its binding mechanism to the umami receptor T1R. *Food Chemistry, 333*, Article 127411. https://doi.org/10.1016/j.foodchem.2020.127411

Chen, Y., Li, P., Liao, L., Qin, Y., Jiang, L., & Liu, Y. (2021). Characteristic fingerprints and volatile flavor compound variations in Liuyang Douchi during fermentation via HS-GC-IMS and HS-SPME-GC-MS. *Food Chemistry, 361*, Article 130055. https://doi.org/10.1016/j.foodchem.2021.130055

Chen, Y. P., Wang, M., Blank, I., Xu, J., & Chung, H. Y. (2021). Saltiness-enhancing peptides isolated from the Chinese commercial fermented soybean curds with potential applications in salt reduction. *Journal of Agricultural and Food Chemistry, 69*(35), 10272–10280. https://doi.org/10.1021/acs.jafc.1c03431

Cui, H., Li, H., Wu, Y., & Hu, X. (2023). Identification, flavor characteristics and molecular docking of umami taste peptides of Xuanwei ham. *Food Research International, 173*, Article 113211. https://doi.org/10.1016/j.foodres.2023.113211

Cui, Z., Zhang, N., Zhou, T., Zhou, X., Meng, H., Yu, Y., … Y.. (2023). Conserved sites and recognition mechanisms of T1R1 and T2R14 receptors revealed by ensemble docking and molecular descriptors and fingerprints combined with machine learning. *Journal of Agricultural and Food Chemistry, 71*(14), 5630–5645. https://doi.org/10.1021/acs.jafc.3c00591

Ding, Y., Li, X., & Kan, J. (2017). Isolation and identification of flavor peptides from douchi (traditional Chinese soybean food). *International Journal of Food Properties, 20*, 1982–1994. https://doi.org/10.1080/10942912.2017.1360906

Du, J., Wang, D., Fan, H., Xu, C., Tai, L., Lin, S., , … Zhao, & Q.. (2021). Structures of human mGlu2 and mGlu7 homo- and heterodimers. *Nature, 594*(7864), 589–593. https://doi.org/10.1038/s41586-021-03641-w

Feng, X., Wang, R., Lu, J., Du, Q., Cai, K., Zhang, B., & Xu, B. (2024). Taste properties and mechanism of umami peptides from fermented goose bones based on molecular docking and molecular dynamics simulation using umami receptor T1R1/T1R3. *Food Chemistry, 443*, Article 138570. https://doi.org/10.1016/j.foodchem.2024.138570

Fu, B., Wu, D., Cheng, S., Xu, X., Zhang, L., Wang, L., , … Du, & M.. (2024). Three novel umami peptides derived from the alcohol extract of the Pacific oyster *(Crassostrea gigas)*: Identification, characterizations and interactions with T1R1/T1R3 taste receptors. *Food Science and Human Wellness, 13*(1), 146–153. https://doi.org/10.26599/FSHW.2022.9250012

Garshick, M. S., Barrett, T. J., Wechter, T., Azarchi, S., Scher, J. U., Neimann, A., … J. S.. (2019). Inflammasome signaling and impaired vascular health in psoriasis. *Arteriosclerosis, Thrombosis, and Vascular Biology, 39*(4), 787–798. https://doi.org/10.1161/ATVBAHA.118.312246

Guo, W., Xiao, Y., Fu, X., Long, Z., Wu, Y., Lin, Q., , … Jiang, & L.. (2023). Identification of novel α-glucosidase and ACE inhibitory peptides from Douchi using peptidomics approach and molecular docking. *Food Chemistry: X, 19*, Article 100779. https://doi.org/10.1016/j.fochx.2023.100779

Guo, W., Zhang, Y., Long, Z., Fu, X., & Ren, K. (2023). Study on the taste active compounds in Douchi using metabolomics method. *Food Chemistry, 412*, Article 135343. https://doi.org/10.1016/j.foodchem.2022.135343

Iwaniak, A., Minkiewicz, P., Darewicz, M., Sieniawski, K., & Starowicz, P. (2016). BIOPEP database of sensory peptides and amino acids. *Food Research International, 85*, 155–161. https://doi.org/10.1016/j.foodres.2016.04.031

Jia, R., Yang, Y., Liao, G., Wu, H., Yang, C., & Wang, G. (2024). Flavor characteristics of umami peptides from Wuding chicken revealed by molecular dynamics simulation. *Journal of Agricultural and Food Chemistry, 72*(7), 3673–3682. https://doi.org/10.1021/acs.jafc.3c08348

Krishna Kumar, K., Wang, H., Habrian, C., Latorraca, N. R., Xu, J., O'Brien, E. S., … B. K.. (2024). Stepwise activation of a metabotropic glutamate receptor. *Nature, 629*(8013), 951–956. https://doi.org/10.1038/s41586-024-07327-x

Lee, D.-K., Ahn, S., Cho, H. Y., Yun, H. Y., Park, J. H., Lim, J., … S. W.. (2016). Metabolic response induced by parasitic plant-fungus interactions hinder amino sugar and nucleotide sugar metabolism in the host. *Scientific Reports, 6*(1), Article 37434. https://doi.org/10.1038/srep37434

Li, C., Hua, Y., Pan, D., Qi, L., Xiao, C., Xiong, Y., , … Zhao, & Y.. (2022). A rapid selection strategy for umami peptide screening based on machine learning and molecular docking. *Food Chemistry, 404*, Article 134562. https://doi.org/10.1016/j.foodchem.2022.134562

Li, J., Wang, W., Liu, J., Li, H., Zhang, N., Yang, F., , … Liu, & Y.. (2021). Human-like performance umami electrochemical biosensor by utilizing co-electrodeposition of ligand binding domain T1R1-VFT and Prussian blue. *Biosensors and Bioelectronics, 193*, Article 113627. https://doi.org/10.1016/j.bios.2021.113627

Lin, S., Han, S., Cai, X., Tan, Q., Zhou, K., Wang, D., , … Wu, & B.. (2021). Structures of Gi-bound metabotropic glutamate receptors mGlu2 and mGlu4. *Nature, 594*(7864), 583–588. https://doi.org/10.1038/s41586-021-03495-2

Liu, H., Da, L.-T., & Liu, Y. (2019). Understanding the molecular mechanism of umami recognition by T1R1-T1R3 using molecular dynamics simulations. *Biochemical and Biophysical Research Communications, 514*(3), 967–973. https://doi.org/10.1016/j.bbrc.2019.05.066

Liu, Q., Gao, X., Pan, D., Liu, Z., Xiao, C., Du, L., , … Zou, & Y.. (2023). Rapid screening based on machine learning and molecular docking of umami peptides from porcine bone. *Journal of the Science of Food and Agriculture, 103*(8), 3915–3925. https://doi.org/10.1002/jsfa.12319

Rapino, F., Zhou, Z., Roncero Sanchez, A. M., Joiret, M., Seca, C., El Hachem, N., … P.. (2021). Wobble tRNA modification and hydrophilic amino acid patterns dictate protein fate. *Nature Communications, 12*(1), 2170. https://doi.org/10.1038/s41467-021-22254-5

Seifert, T., Malo, M., Lengqvist, J., Sihlbom, C., Jarho, E. M., & Luthman, K. (2016). Identification of the binding site of Chroman-4-one-based Sirtuin 2-selective inhibitors using Photoaffinity labeling in combination with tandem mass spectrometry. *Journal of Medicinal Chemistry, 59*(23), 10794–10799. https://doi.org/10.1021/acs.jmedchem.6b01117

Shen, Y., Maupetit, J., Derreumaux, P., & Tufféry, P. (2014). Improved PEP-FOLD approach for peptide and Miniprotein structure prediction. *Journal of Chemical Theory and Computation, 10*(10), 4745–4758. https://doi.org/10.1021/ct500592 m

Shirotani, N., Bygvraa Hougaard, A., Lametsch, R., Agerlin Petersen, M., Rattray, F. P., & Ipsen, R. (2021). Proteolytic activity of selected commercial *Lactobacillus helveticus* strains on soy protein isolates. *Food Chemistry, 340*, Article 128152. https://doi.org/10.1016/j.foodchem.2020.128152

Singh, S. K., Upadhyay, A. K., & Reddy, M. S. (2021). Screening of potent drug inhibitors against SARS-CoV-2 RNA polymerase: An in silico approach. *3 Biotech, 11*(2), 93. https://doi.org/10.1007/s13205-020-02610-w

Smith, A., Dong, X., & Raghavan, V. (2022). An overview of molecular dynamics simulation for food products and processes. *Processes, 10*(1), 1. https://doi.org/10.3390/pr10010119

Su, G., Yu, Z., Wang, H., Zhao, M., Zhao, T., & Zhang, J. (2023). Impact of ternary NADES prepared from proline, glucose and water on the Maillard reaction: Reaction activity, Amadori compound yield, and taste-enhancing ability. *Food Chemistry: X, 20*, Article 100905. https://doi.org/10.1016/j.fochx.2023.100905

Wang, C., Wu, Y., Xiang, H., Chen, S., Zhao, Y., Cai, Q., , … Wang, & Y.. (2024). In-depth discovery and taste presentation mechanism studies on umami peptides derived from fermented sea bass based on peptidomics and machine learning. *Food Chemistry, 448*, Article 138999. https://doi.org/10.1016/j.foodchem.2024.138999

Wang, H., Wang, W., Zhang, S., Hu, Z., Yao, R., Hadiatullah, H., Li, P., & Zhao, G. (2023). Identification of novel umami peptides from yeast extract and the mechanism against T1R1/T1R3. *Food Chemistry, 429*, Article 136807. https://doi.org/10.1016/j.foodchem.2023.136807

Wang, X., Wang, M., Xu, T., Feng, Y., Shao, Q., Han, S., , … Wu, & B.. (2023). Structural insights into dimerization and activation of the mGlu2-mGlu3 and mGlu2-mGlu4 heterodimers. *Cell Research, 33*(10), 762–774. https://doi.org/10.1038/s41422-023-00830-2

Wang, Y., Xiang, F., Zhang, Z., Hou, Q., & Guo, Z. (2021). Characterization of bacterial community and flavor differences of different types of Douchi. *Food Science & Nutrition, 9*(7), 3460–3469. https://doi.org/10.1002/fsn3.2280

Wayment-Steele, H. K., Ojoawo, A., Otten, R., Apitz, J. M., Pitsawong, W., Hömberger, M., … D.. (2024). Predicting multiple conformations via sequence clustering and AlphaFold2. *Nature, 625*(7996), 832–839. https://doi.org/10.1038/s41586-023-06832-9

Yan, H., Li, W. X., Zhu, Y. L., Lin, Z. Y., Chen, D., Zhang, Y., … Y.. (2024). Comprehensive comparison of aroma profiles and chiral free and glycosidically bound volatiles in Fujian and Yunnan white teas. *Food Chemistry, 448*, Article 139067. https://doi.org/10.1016/j.foodchem.2024.139067

Yang, F., Fu, A., Meng, H., Liu, Y., & Bi, S. (2024). Non-volatile taste active compounds and umami evaluation of Agrocybe aegerita hydrolysates derived using different enzymes. *Food Bioscience, 58*, Article 103772. https://doi.org/10.1016/j.fbio.2024.103772

Zhang, J., Tu, Z., Wen, P., Wang, H., & Hu, Y. (2024). Peptidomics screening and molecular docking with umami receptors T1R1/T1R3 of novel umami peptides from oyster (*Crassostrea gigas*) hydrolysates. *Journal of Agricultural and Food Chemistry, 72*(1), 634–646. https://doi.org/10.1021/acs.jafc.3c06859

Zhang, L., Pu, D., Zhang, J., Hao, Z., Zhao, X., Sun, B., & Zhang, Y. (2023). Identification of novel umami peptides in chicken breast soup through a sensory-guided approach and molecular docking to the T1R1/T1R3 taste receptor. *Journal of Agricultural and Food Chemistry, 71*(20), 7803–7811. https://doi.org/10.1021/acs.jafc.3c01251

Zhang, L., Zhang, L., Pérez-Moreno, J., Bin, L., Zhang, F., & Yu, F. (2024). Novel umami peptides from two *Termitomyces* mushrooms and molecular docking to the taste receptor T1R1/T1R3. *Food Science and Human Wellness, 13*(2), 1055–1064. https://doi.org/10.26599/FSHW.2022.9250091

Zhao, D., Lu, K., Liu, G., Hou, J., Yuan, L., Ma, L., , … He, & J.. (2020). PEP-FOLD design, synthesis, and characteristics of finger-like polypeptides. *Spectrochimica Acta Part A: Molecular and Biomolecular Spectroscopy, 224*, Article 117401. https://doi.org/10.1016/j.saa.2019.117401

Zhao, W., Su, L., Huo, S., Yu, Z., Li, J., & Liu, J. (2023). Virtual screening, molecular docking and identification of umami peptides derived from *Oncorhynchus mykiss*. *Food Science and Human Wellness, 12*(1), 89–93. https://doi.org/10.1016/j.fshw.2022.07.026